Necrotic Tissue Distribution Analysis: Preliminary Investigation for Reducing Necrosis Overestimation in Intravascular Ultrasound Virtual Histology Images

Fernando JR Sales[1], Breno AA Falcão[2] , João LAA Falcão[3] , Sergio S Furuie[4], Pedro A Lemos[2]

[1] Núcleo de Telessaúde da Universidade Federal de Pernambuco (NUTES-UFPE), Recife, Brazil
[2] Heart Institute (InCor) - Hospital das Clínicas da Faculdade de Medicina da USP, São Paulo, Brazil
[3] University of Fortaleza Medical School (UNIFOR), Fortaleza, Brazil
[4] Biomedical Engineering Lab - Escola Politécnica da USP, São Paulo, Brazil

Abstract

Background: The intravascular ultrasound (IVUS) Virtual Histology (VH) classifies the atherosclerotic plaque components, according to four classes – fibrous (FT), fibrofatty (FF), dense calcium (DC), and necrotic tissue (NC). Past works have proven a possible overestimation of necrotic content in VH images, particularly when NC is confluent to DC. Additionally, NC has been used as a severity marker for atherosclerotic plaque. Aiming to observe a possible correction rule for overestimation problem, an experiment was designed. Eight patients have been submitted to stent implantation (PCI). VH examinations have been performed before (PRE) and after (POS) PCI, totalizing more than 300 frames. NC content was divided into two classes: RW and RP, which corresponds, respectively, to NC confluent to DC and not confluent. Grayscale IVUS images were processed to extract normalized intensity histograms according to NC classification. Differences between intensity distributions RW and RP necrotic tissue were found, which may be useful to be considered to minimize overestimation of necrosis in VH images. These preliminary results encourage further investigation with larger sample sizes for proposing correction-imaging methods.

1. Introduction

The intravascular ultrasound (IVUS) Virtual Histology (VH) classifies the atherosclerotic plaque components, according to four classes – fibrous (FT), fibrofatty (FF), dense calcium (DC), and necrotic tissue (NC) [1]. Several studies have been using VH-IVUS as a reference method for in-vivo plaque composition assessment [2-4].

In the last two decades, several efforts have been made in order to identify markers and plaque features associated to sudden death or major adverse coronary events (MACE) [5]. Certain lesions were directly associated with an increased risk for sudden death, acute myocardial infarction among other severe events [6]. Thin Cap Fibroatheroma was classified as lesions containing lipid pools close to the luminal wall and separated by a thin fibrotic cap being associated with a higher rupture risk [6].

Past works have proven a possible overestimation of necrotic content in VH images, particularly when NC is confluent to DC [7,8].

Once NC component has been associated to several MACE's and has an overestimation in VH IVUS, we decided to study NC behavior in order to identify features possible to use to underestimate misclassification necrotic content in VH images.

2. Materials and methods

2.1. Study protocol

The present study used data from a prospective essay which included a group of 8 patients who underwent successful single stent implantation (PCI) (<30% residual stenosis with normal antegrade flow by angiography), for which high quality VH-IVUS examination was obtained at baseline (pre-PCI) and at the end of the procedure (post-PCI). All lesions were treated with the same stainless steel stent type (Apolo®, Cordynamic, Barcelona, Spain [strut thickness 0.0045"]). Patients with visible thrombus or intraluminal haziness at angiography, acute myocardial infarction < 48 hours or unstable angina with rest pain < 48 hours were excluded from analysis.

The local ethics committee approved the study protocol and written informed consent was obtained from every patient.

2.2. Materials

In this work, more than 300 VH frames have been used in total. For every lesion, composition (VH-IVUS) and

grey scale (GS-IVUS) images have been paired allowing a frame-to-frame association between grey scale features and composition information. Necrotic Core (NC) and Dense Calcium (DC) binary masks have been extracted from VH images as described in [9]. Additionally, NC components were classified according to their neighborhood: RW and RP, which corresponds, respectively, to NC confluent to DC and not confluent.

Image processing tools have been developed in Java [9], using Eclipse IDE and ImageJ (IJ) together. Image processing methods utilized have been described in [8,9].

2.3. Methods

Grey scale (GS) pixel intensity distribution has been assessed for necrotic content in every lesion for further analysis. Intensity histograms have been extracted and normalized to obtain unitary area distributions, such as probability density functions.

After compiling information from images, some comparisons have been performed in order to identify possible differences between necrotic content groups. RW and RP intensity histograms have been directly compared, according to PCI status: PRE or POS. Mann-Whitney U test was used in the matched comparison between RW and RP distributions.

After that, some additional metrics to quantify distance between distributions were calculated and are shown in Table 1. Some works have related that paired comparisons like paired T-test may be not the best way to assess the distance between distributions because of their sensitivity to histograms translations, for example.

3. Results

This work has used the same database assessed in [9]. In that paper, we concluded that VH overestimates NC content, especially when there are DC components related to necrotic content. The overestimated amount is possible caused for a misclassification error, inherent to VH classification algorithm. Based on MW-UT results shown in Table 2, RW and RP distributions are different for every patient, before and after stent implantation. Despite of the significance of these findings, some additional metrics were calculated to possibly identify issues related to RP and RW intensity distributions.

According to Fig. 1, RP and RW distributions for patient "7" were visually different. RW histogram has presented a bimodal shape, with intensity values around 200, which were uncommon on RP histogram.

Table 1. Distance measures between distributions used in this work.

Distance Measure	Equation
Bhattacharrya Distance	$D_{Bha}(p_1,p_2) = \sqrt{1-\sum_{i=0}^{255} p_1(i)p_2(i)}$
Kullback-Leiber Divergence	$D_{KL}(p_1,p_2) = KL(p_1,p_2) + KL(p_2,p_1)$
Jenson-Shannon Divergence	$D_{KL}(p_1,p_2) = KL(p_1,q) + KL(p_2,q)$, where $q(i) = \frac{p_1(i)+p_2(i)}{2}$
Earth Mover Distance [1]	$EMD(p_1,p_2) = \sum_{i=0}^{255} \lvert C_{p_1}(i) - C_{p_2}(i) \rvert$

Where: $\mathrm{KL(u,v)} = \sum_{i=0}^{255} \mathrm{u(i)} \ln \frac{\mathrm{u(i)}}{\mathrm{v(i)}}$, $C_{p_1}(i) = \sum_{k=0}^{i} p_1(k)$

Observing the mathematical definitions for metrics on Table 1, an inference has been performed. BHA distance assume null value if distributions are identical and tending to ONE whether their differences increases. KLD, JSD and EMD tend to ZERO whether the normalized distributions become identical, with values increasing otherwise [10].

Results from table 3 shows that RP and RW histograms distribution increases after stent implantation, because of artifactual NC content added to VH images. Histogram changes are related to an increment of pixels with gray scale intensity around 200, which is pretty uncommon for RP pixels.

Table 2. Mann-Whitney U Test (MW-UT) for comparing RP and RW distributions for each patient, according to PCI status: PRE and POS. For this test, the significance level was 0.05 (alpha).

Patient Label	p-Value for RP and RW distributions comparison using MW-UT.			
	PRE-PCI		POS-PCI	
7	5.3e-04	P<0.05	1.5e-02	P<0.05
11	2.4e-03	P<0.05	1.8e-04	P<0.05
18	4.3e-03	P<0.05	3.7e-10	P<0.05
27	1.2e-03	P<0.05	1.8e-07	P<0.05
37	9.3e-04	P<0.05	2.6e-05	P<0.05
43	5.8e-04	P<0.05	3.2e-03	P<0.05
48	2.1e-07	P<0.05	1.5e-07	P<0.05
58	2.1e-06	P<0.05	4.0e-04	P<0.05

4. Discussion

This work has used the same database assessed in [8]. In that paper, we concluded that VH overestimates NC content, especially when there are DC components related to necrotic content. The overestimated amount is possible caused for a misclassification error, inherent to VH

[1] In this case, Earth Mover Distance is simplified as shown in Table 1. General explanation is available in [11].

classification algorithm.

However, based on artifactual relationship between necrosis and dense calcium, we decided to check whether "pure" NC and NC confluent to DC presents the same features in GS IVUS images.

In our results, differences between RP and RW were observed for every patient, with significance for some patients. These findings are original and may point to a new route in order to identify NC content more prone to be a misclassified pixel. This investigation should guide us to a new methodology for necrosis quantification and a new possibility for VH examinations' analysis.

Comparison between RP and RW components shows a presence of some RW pixels with higher intensity than those presents in RP distribution. A possible novel hypothesis to be designed is related to those high intensity NC pixels presented post-intervention and confluent to dense calcium. Suppose that overestimated necrosis would be these one with higher intensity, a hypothesis test should be designed to re-label NC content as "artifactual necrosis" (AN).

These further analyses should provide a modern analysis, which allows VH studies to assess necrotic content into intervals instead of absolute values. Whether these analyses lead us to reliable conclusions, several studies will be re-studied over this novel VH methodology.

A critical point of described analysis is related to its validation. Histopathological analysis (HA) has been still gold standard method for plaque classification. Unfortunately, a clinical essay evolving HA of coronary arteries specimens should not be performed in vivo. In addition, there are several costs and difficulties associated to this study design.

5. Conclusions

Based on presented methodology, data and results there are significant differences between GS intensity distribution for RP and RW necrotic contents. Several previous studies pointed to an overestimation of necrotic tissue around dense calcium content in VH images.

We hope that some kind of correction model or a method to underestimate NC in VH images by means of the GS intensity distribution. Future steps will be focused in the analyses of intensity histograms in order to propose a novel "correction" rule which permits a reduction in NC content, especially in which cases with several NC connected to DC pixels.

Acknowledgements

Thanks for FAPESP which provided several resources for the VH IVUS images. We would like to thank the CNPq for supporting this work – CNPq. 486769/2012-7.

References

[1] Nair A, Kuban BD, Tuzcu EM, Schoenhagen P, Nissen SE, Vince DG. Coronary plaque classification with intravascular ultrasound radiofrequency data analysis. Circulation 2002; 106:2200 - 2206.

[2] Konig A, Klauss V. Virtual histology. Heart 2007; 93: 977-982.

[3] Xiaofan W et al. Virtual histology intravascular ultrasound analysis of non-culprit attenuated plaques detected by grayscale intravascular ultrasound in patients with acute coronary syndromes. The American Journal of Cardiology 2010;105:48-53.

[4] Deliargyris EN, Intravascular ultrasound virtual histology derived thin cap fibroatheroma: now you see it, now you don't…. Journal of the American College of Cardiology 2010;55:1598-1599.

[5] Naghavi M, et al. From vulnerable plaque to vulnerable patient: a call for new definitions and risk assessment strategies: Part I. Circulation 2003; 108: 1664-72.

[6] Virmani R, et al. Pathology of the vulnerable plaque. J Am Coll Cardiol 2006; 47: C13-8.

[7] Sales FJR, Falcao JLAA, Falcao BAA, Lemos PA, Furuie SS. Evidences of possible necrotic-core artefact around dense calcium in Virtual Histology images. Computers in Cardiology 2008; 35; 545-548.

[8] Sales FJR, et al. Evaluation of plaque composition by intravascular ultrasound "virtual histology": the impact of dense calcium on the measurement of necrotic tissue. Eurointervention, 2010: 6; 394-399.

[9] Sales FJR, Falcao JLAA, Falcao BAA, Lemos PA, Furuie SS. A Computational Tool for Coronary Atherosclerotic Plaque Analysis of Virtual Histology Images. Computers in Cardiology 2010; 37; 907-10.

[10] Cha S-H. Comprehensive survey on distance/similarity measures between probability density functions. City 2007;1.2: 1.

[11] Ling H et al. An efficient earth mover's distance algorithm for robust histogram comparison. European Conference on Computer Vision (ECCV), LNCS 3953. 2006; III:330-343.

Address for correspondence.

Name. Fernando J R Sales.
Full postal address. NUTES – Hospital das Clínicas/UFPE. 2o andar. Av Prof Moraes Rego, s/n. Cidade Universitária, Recife, PE, Brazil.
E-mail address (optional). fernando.sales@ ufpe.br

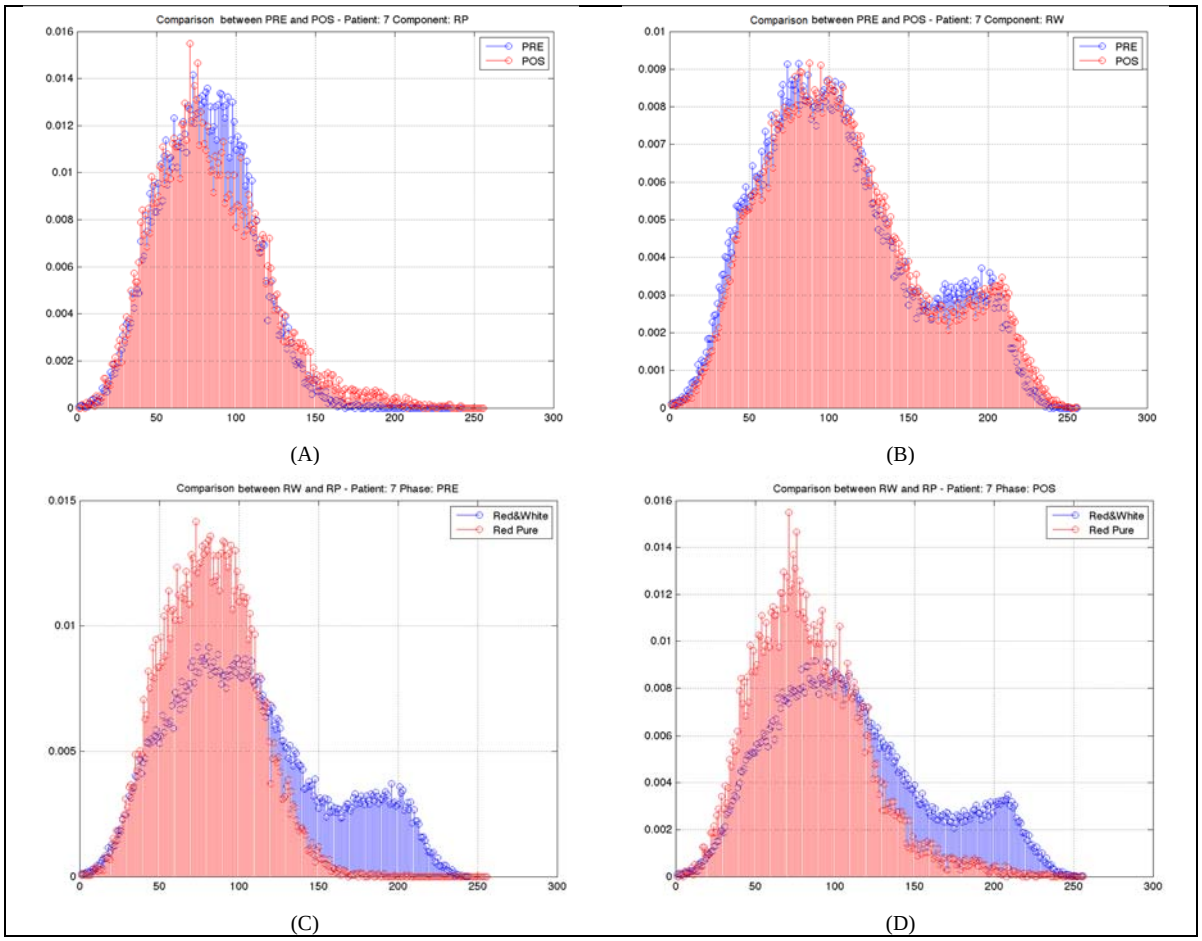

Fig. 1 – Normalized histograms for NC content for a patient, named as "Patient 7", and respective comparisons. (A): PRE and POS distributions were displayed for RP. (B): PRE and POS distributions were displayed for RW. (C): RW and RP distributions for PRE-PCI group and (D) RW and RP distributions for POS-PCI group. There are some observable differences in each one of displayed images.

Table 3. Distance and divergence metrics used for comparing differences between NC intensity distributions. Metrics used are described on Table 1.

Patient Label	RP and RW distances – PRE-PCI				RP and RW distances – POS-PCI			
	BHA	KLD	JSD	EMD	BHA	KLD	JSD	EMD
7	0.31	2.48	0.11	25.52	0.25	0.62	0.08	26.8
11	0.26	0.84	0.09	18.16	0.30	2.31	0.11	27.41
18	0.25	0.63	0.08	21.45	0.40	4.22	0.19	32.86
27	0.24	0.99	0.07	20.25	0.40	5.32	0.18	28.42
37	0.23	0.82	0.07	18.43	0.30	2.33	0.10	24.66
43	0.20	0.66	0.05	17.37	0.27	1.26	0.09	22.26
48	0.33	2.11	0.13	30.27	0.35	2.89	0.14	31.61
58	0.28	1.11	0.10	22.54	0.29	1.31	0.11	26.55
Patient Label	RP PRE and RP POS distances				RW PRE and RW POS distances			
	BHA	KLD	JSD	EMD	BHA	KLD	JSD	EMD
7	0.12	0.30	1.9e-02	4.08	0.06	0.04	5.8e-03	4.03
11	0.10	0.13	1.4e-02	2.54	0.15	0.42	3.0e-03	9.80
18	0.27	1.38	9.3e-03	17.24	0.12	0.07	1.8e-02	8.19
27	0.28	2.14	9.0e-02	7.23	0.09	0.06	1.3e-02	6.28
37	0.10	0.20	1.3e-02	0.57	0.08	0.05	9.4e-03	6.67
43	0.22	0.38	7.3e-02	18.38	0.18	0.21	4.8e-02	22.84
48	0.08	0.12	8.5e-03	0.67	0.04	0.01	2.8e-03	2.29
58	0.16	0.27	3.5e-02	10.25	0.14	0.11	2.7e-02	14.25